The Journal of Chemical Physics ARTICLE scitation.org/journal/jcp

Correlation consistent basis sets designed for density functional theory: Second-row (Al-Ar)

Cite as: J. Chem. Phys. 151, 064110 (2019); doi: 10.1063/1.5113873
Submitted: 8 June 2019 • Accepted: 16 July 2019 •
Published Online: 9 August 2019

Andrew Mahler,[1] John J. Determan,[2,a)] and Angela K. Wilson[3,b)]

AFFILIATIONS

[1] Department of Chemistry and Center for Advanced Scientific Computing and Modeling, University of North Texas, Denton, Texas 76203-5017, USA
[2] Department of Chemistry, Western Illinois University, Macomb, Illinois 61455, USA
[3] Department of Chemistry, Michigan State University, East Lansing, Michigan 48824, USA

[a)] **Electronic mail:** jj-determan@wiu.edu
[b)] **Electronic mail:** akwilson@msu.edu

ABSTRACT

The cc-pV(n+d)Z correlation consistent basis sets of double- through quintuple-ζ quality for the atoms Al-Ar have been modified for use with density functional theory (DFT). These basis set modifications include truncation of high-angular momentum basis functions, recontraction of the *s*- and *p*-functions, and reoptimization of basis function exponents with generalized gradient approximation and hybrid-DFT functionals. The effects of basis set truncation, recontraction, and reoptimization are shown to improve convergence behavior in atomic energies as well as dissociation energies and enthalpies of formation.

I. INTRODUCTION

Density functional theory (DFT) methods, in particular those which are based on theories developed by Kohn and Sham,[1] are among the most popular electronic structure methods developed.[2–8] The success of Kohn-Sham based DFT methods can be directly traced to their low computational cost in comparison to *ab initio* wavefunction methods, as the effects of electron correlation in Kohn-Sham DFT methods are primarily accounted for through the exchange correlation functional, V_{XC}, rather than through excitations of electrons into the virtual orbitals of a reference state.

Gaussian basis sets are widely used in solving density functional computations; however, most of the basis sets used in these computations are sets that were constructed using Hartree-Fock and post-Hartree-Fock methods rather than density functional methods. In fact, *ab initio*-derived basis sets can be highly effective and, in many cases, even more so than basis sets designed for DFT.[9–13] One of the most widely used families of basis sets for both *ab initio* and density functional calculations is the correlation consistent basis set family. These sets have been designed using *ab initio* methods and are based upon the systematic accounting of correlation energy. An important feature of these basis sets, which results from their unique construction, is that a number of properties, such as energies and bond lengths, converge to a limit with respect to increasing basis set level for *ab initio* methods. The limit—known as the complete, infinite, or saturated basis set limit—is the limit at which no further improvements to the basis set can improve upon the results. At this limit, the only source of error in the calculation is the error *intrinsic to the method*.

Correlation consistent basis sets are useful for the calculation of properties such as atomization energies and geometries of molecules. While these sets slowly converge toward the complete basis set limit for properties such as these for *ab initio* methods, the convergence to a limit occurs much more quickly for DFT methods. However, the combination of DFT with correlation consistent basis sets—which were designed for use with *ab initio* methods—does not always result in a limit that is in good agreement with experimental values or other high level theoretical methods, nor does systematic convergence to a limit for the properties with increasing basis set necessarily occur.[11] This lack of systematic convergence of the correlation consistent basis sets when used with DFT

methods is of particular importance, as this convergence provides a vital route for the elimination of error arising from basis set incompleteness as well as for an understanding of the error arising from the choice of an applied method. Because density functional methods account for electron correlation in a different manner than *ab initio* methods, the requirements for a suitably optimized one-electron basis set for Kohn-Sham density functionals may be different than those of Hartree-Fock based wavefunction methods.

This prior concern is what led Jensen to develop a family of basis sets called the polarization consistent basis sets (pc-*n*) which were designed explicitly for DFT methods.[14–18] These sets are akin to the correlation consistent basis sets in that they were constructed in a systematic way, though they were built upon the idea of angular momentum functions decreasing geometrically [i.e., ns(n/2)p(n/4)d(n/8)f] rather than decreasing arithmetically as is the case with the correlation consistent basis sets. As a consequence, the pc-3 and p-4 basis sets have more *s* and *p* basis functions than analogously sized cc-pVQZ and cc-pV5Z basis sets. The intent of the pc sets was to provide a family of sets that were more suitable, in principle, than *ab initio*-based sets, with the potential promise of improved property predictions relative to post-HF sets like the correlation consistent basis sets.

In a study by Wang and Wilson, however, it was shown that the pc-n basis sets, despite being optimized for use with DFT methods, did not generally provide better atomization energies than the correlation consistent basis sets, nor did they result in smooth convergence toward the Kohn-Sham (KS) limit (analogous to the CBS limit for wavefunction-based methods) for these energies. Furthermore, the differences in the calculated atomization energies between the pc-*n* and cc-pV*n*Z sets were shown to be less than 1 kcal mol^{-1}. This similarity in energies arising from the pc-*n* and cc-pV*n*Z sets is especially significant, as the pc-*n* sets include equal or more basis functions than the corresponding cc-pV*n*Z sets, including high angular momentum basis functions (e.g., *f*-, *g*-, and *h*-functions), as shown in Table I. While the exciting aspect of the polarization consistent basis set is that the work demonstrated that there is more than one route to achieve energies similar to those of the correlation consistent basis sets, it is important to note that *ab initio* developed basis sets are quite suitable for DFT calculations.

Even given the observation that the correlation consistent basis sets are suitable for DFT calculations, however, these basis sets can be improved or better "tuned" to improve efficiencies as well as gain better convergence behavior of properties toward the KS limit. To improve efficiency, Wilson *et al.* investigated the need for higher angular momentum functions. In studies by Prascher *et al.*, it was shown that, when using DFT methods, the truncation of the *g*- and *h*-functions from the correlation consistent basis sets resulted in deviations in ionization energies and electron affinities of less than 0.01 eV and dissociation energies by less than 1 kcal mol^{-1} for many atomic and molecular systems. Furthermore, as shown by Prascher and Wilson,[19] recontracting the *s*- and *p*-functions of the cc-pV*n*Z sets to fit the occupied Kohn-Sham orbitals in an analogous manner to the contraction of the basis set exponents to the Hartree-Fock orbitals in the original cc-pV*n*Z method can improve the convergence of the molecular ionization potential and electron affinities compared to the same properties calculated with conventional correlation consistent sets. The convergence of molecular atomization energies toward the Kohn-Sham limit with recontracted correlation consistent basis sets, however, was only improved by also including basis set superposition error (BSSE) corrections. As shown by Gibson, improvement for computations involving density functionals could be achieved by reoptimizing the correlation consistent basis sets.[20]

TABLE I. (a) The composition of basis set primitive and contracted functions for the cc-pV(*n* + d)Z and pc-*n* basis sets for second row atom (Al-Ar) sets. (b) Basis set primitive and contracted function compositions for the recontracted and reoptimized correlation consistent basis sets are shown.

	Primitives	Contracted functions
(a)		
cc-pV(D + d)Z	12*s*8*p*2*d*	4*s*3*p*2*d*
cc-pV(T + d)Z	15*s*9*p*3*d*1*f*	5*s*4*p*3*d*1*f*
cc-pV(Q + d)Z	16*s*11*p*4*d*2*f*1*g*	6*s*5*p*4*d*2*f*1*g*
cc-pV(5 + d)Z	20*s*12*p*5*d*3*f*2*g*1*h*	7*s*6*p*5*d*3*f*2*g*1*h*
pc-1	11*s*8*p*1*d*	4*s*3*p*1*d*
pc-2	13*s*10*p*2*d*1*f*	5*s*4*p*2*d*1*f*
pc-3	17*s*13*p*4*d*2*f*1*g*	6*s*5*p*4*d*2*f*1*g*
pc-4	21*s*16*p*6*d*3*f*2*g*1*h*	7*s*6*p*6*d*3*f*2*g*1*h*
(b)		
cc-p[rt(o)]VDZ	12*s*8*p*2*d*	4*s*3*p*2*d*
cc-p[rt(o)]VTZ	15*s*9*p*3*d*1*f*	5*s*4*p*3*d*1*f*
cc-p[rt(o)]VQZ	16*s*11*p*4*d*2*f*	6*s*5*p*4*d*2*f*
cc-p[rt(o)]V5Z	20*s*12*p*5*d*3*f*	7*s*6*p*5*d*3*f*

Based upon these prior studies, it does not appear that high-angular momentum functions contribute significantly to the performance of DFT methods for the prediction of properties, such as atomization energies, ionization potentials, and electron affinities of "typical" main group (pre-d-block) molecules, and instead, provide an unnecessary computational sink. Second, much of the nonsystematic behavior of correlation consistent basis sets when used with DFT methods appears to stem from the basis set contractions and basis set superposition error arising from the correlation consistent basis sets' construction for Hartree-Fock and post-Hartree-Fock methods. A question arises, however, as to whether complete reoptimization *and* recontraction of the correlation consistent basis sets can aid systematic convergence behavior of correlation consistent basis sets when used with DFT methods.

Encouraged by the improvements in computational efficiency and better convergence that has been observed in prior studies, the current study seeks to improve correlation consistent basis sets for DFT calculations involving second-row species.[20] Several approaches are considered in the modification of basis sets including reoptimization, recontraction, and truncation of basis sets for use with DFT methods. In Secs. II and III, approaches for the construction of a series of correlation consistent basis sets designed for

DFT approaches for second row atoms (Al-Ar) are discussed, and computed bond lengths and enthalpies of formation for second row containing molecules are presented.

II. METHODOLOGY

The cc-pV(n+*d*)Z basis sets of Dunning, Peterson, and Wilson serve as the initial basis sets in this study.[21] In 2001, these sets were recommended as the appropriate correlation consistent basis sets for second-row main group atoms, replacing the original correlation consistent sets, which were deemed to be lacking, with near duplication of exponents in the *d* sets and lack of sufficient high-exponent functions.[22–25] Improvement in convergence was obtained by augmenting and reoptimizing the set, including tight-*d* basis set functions.

All calculations in this work were performed using common density functionals: BLYP and B3LYP.[26–28] Exponent optimizations were performed, and contraction coefficients were determined using the MOLPRO suite of quantum chemistry computational software.[29] Dissociation energies and enthalpies of formation at zero kelvin were calculated using the Gaussian09 computational suite.[30] Exponent optimizations were performed using the Broyden–Fletcher–Goldfarb–Shanno (BFGS) method and an orbital gradient threshold of 1×10^{-6} as implemented in the MOLPRO software suite. Radial distribution functions were calculated using the GAMESS software package.[31,32]

The truncation of the correlation consistent basis sets for DFT methods was performed in the same manner as previously demonstrated by Prascher *et al.*[33] where the *g*- and *h*-functions were removed from the cc-pVQZ and cc-pV5Z sets. The recontractions of the *s*- and *p*-functions were performed using the general contraction scheme of Raffenetti,[34] but with Kohn-Sham orbital coefficients used *in lieu* of Hartree-Fock coefficients. For S and Cl, two sets of contraction coefficients for the 3*p* orbital exist: the singly occupied p eigenstate and doubly occupied p eigenstate. Similar to the recontraction study by Prascher and Wilson for the first row elements, the doubly occupied Kohn-Sham orbital coefficients were used for the second row elements. For example, in sulfur, the p electronic configuration is $p_x^2 p_y p_z$. The contraction coefficient of the doubly occupied (p_x^2) atomic orbital was utilized.

The DFT recontracted and reoptimized basis sets for the atoms H, B-Ar developed by Gibson were also employed in this work.[20] In studies by Prascher *et al.*, it was found that though recontraction of the first-row element basis sets improved convergence, it did not lead to smooth monotonic convergence in all cases.[19] For the first-row atoms, Gibson examined additional modifications to the basis sets of first-row atoms and examined the applicability of revised DFT-based basis sets for combustion energies. Specifically, in addition to truncations and recontractions, the first-row basis sets were reoptimized with respect to the *s*, *p*, *d*, and *f* primitives in logarithmic space with respect to the minimization of the KS energy utilizing the BFGS algorithm, as detailed above. Here, we consider the utility of a number of modifications—a redesign—of the basis sets as the electronic structure and basis set become more complicated/larger. Optimizations of the correlation consistent exponents were performed on the ground states of the atoms Al-Ar, using the same method employed in the original optimization of the exponents for the correlation consistent basis sets.[35] In particular, *s*, *p*, *d*, and *f* primitives of the cc-pVnZ basis sets were reoptimized in logarithmic space to minimize either BLYP or B3LYP energies using the Broyden-Fletcher-Goldfarb-Shanno (BFGS) algorithm.

To differentiate these new basis sets from previous correlation consistent basis sets, the recontracted and truncated basis sets have been noted as cc-p[rt(λ)]V*n*Z—hereafter also referred to as *recontracted*—while the optimized, recontracted, and truncated basis sets—hereafter referred to as *reoptimized*—have been noted as cc-p[rt(o-λ)]V*n*Z, where λ is the functional for which the basis set was recontracted and/or reoptimized. This notation will be used throughout this work. The composition of basis set primitive and contracted functions for the resulting recontracted and reoptimized correlation consistent basis sets is shown in Table I. Both the first-row element (which were developed by Gibson and are utilized in the current study) and the second-row element basis sets are included in the supplementary material for convenience.

Ground state energies, homonuclear dissociation energies, and equilibrium bond lengths for second row species were calculated using the conventional cc-pV(*n* + d)Z basis sets as well as the recontracted and reoptimized sets of this work. In order to approximate the Kohn-Sham limit when basis set convergence is illustrated, two extrapolation schemes developed for wavefunction-based methods have been used. While other extrapolation schemes may be used for extrapolations of properties to the Kohn-Sham limit, these two schemes have been used in previous studies involving reoptimization of the cc-pVnZ basis sets for density functional computations of first row species. In these schemes, the TZ and QZ level basis sets are the highest basis set levels used, as these schemes will be more practical for extrapolating the properties of larger molecules. The first scheme is the three-point, mixed-Gaussian extrapolation formula of Peterson *et al.*,[36]

$$E_n = E_{KS} + Ae^{-(n+1)} + Be^{-(n+1)^2}. \quad (1)$$

The second scheme employed in this work is the Schwartz inverse cubic formula,[37]

$$E_n = E_{KS} + \frac{A}{(l_{max})^3}. \quad (2)$$

For both extrapolation schemes, E_n indicates the energy calculated using the associated *n*th level basis set and E_{KS} is the Kohn-Sham limit. In the inverse Schwartz formula, the *n*th level basis set also serves as the l_{max} for the formula. However, for the truncated basis sets, the *g*- and *h*-functions have also been truncated from the quadruple-ζ or quintuple-ζ basis sets.

III. RESULTS

A. Atomic energies and radial distribution functions

Calculations of atomic energies using cc-pV(*n* + d)Z, cc-p[rt(λ)]V*n*Z, and cc-p[rt(o-λ)]V*n*Z were performed with both BLYP and B3LYP functionals, the results of which are found in Tables II and III. For both the recontracted and reoptimized

TABLE II. Atomic ground state energies calculated with the BLYP functional for the atoms Al-Ar are given. All energies are in hartrees (E_H).

		Basis set		
Atom	n	cc-pV(n + d)Z	cc-p[rt(BLYP)]VnZ	cc-p[rt(o-BLYP)]VnZ
Al	D	−242.367 774	−242.376 057	−242.376 695
	T	−242.375 187	−242.381 850	−242.381 985
	Q	−242.380 339	−242.383 434	−242.383 491
	5	−242.382 075	−242.383 730	−242.383 804
	P	−242.383 34	−242.384 36	−242.384 37
	S3	−242.384 10	−242.384 59	−242.384 59
Si	D	−289.372 358	−289.380 417	−289.380 900
	T	−289.380 918	−289.387 091	−289.387 314
	Q	−289.384 217	−289.389 441	−289.389 528
	5	−289.388 328	−289.389 778	−289.389 794
	P	−289.386 14	−289.390 81	−289.390 82
	S3	−289.386 62	−289.391 16	−289.391 14
P	D	−341.257 928	−341.266 235	−341.267 099
	T	−341.268 518	−341.274 316	−341.274 685
	Q	−341.271 715	−341.277 189	−341.277 324
	5	−341.276 263	−341.277 595	−341.277 665
	P	−341.273 57	−341.278 86	−341.278 86
	S3	−341.274 05	−341.279 29	−341.279 25
S	D	−398.106 858	−398.115 402	−398.116 348
	T	−398.121 836	−398.127 442	−398.127 921
	Q	−398.125 486	−398.130 942	−398.131 094
	5	−398.130 169	−398.131 478	−398.131 605
	P	−398.127 61	−398.132 98	−398.132 94
	S3	−398.128 15	−398.133 50	−398.133 41
Cl	D	−460.139 499	−460.148 782	−460.149 810
	T	−460.157 363	−460.162 893	−460.162 437
	Q	−460.161 479	−460.166 847	−460.167 001
	5	−460.165 934	−460.167 412	−460.167 587
	P	−460.163 87	−460.169 15	−460.169 66
	S3	−460.164 48	−460.169 73	−460.170 33
Ar	D	−527.521 045	−527.531 162	−527.532 327
	T	−527.540 243	−527.545 762	−527.546 399
	Q	−527.544 725	−527.550 039	−527.550 214
	5	−527.548 722	−527.550 748	−527.550 827
	P	−527.547 33	−527.552 53	−527.552 43
	S3	−527.548 00	−527.553 16	−527.553 00

sets, energy recovery was seen to be improved compared to the cc-pV(n + d)Z sets, with an average energy reduction of 5.43, 3.69, 3.13, and 0.97 kcal mol^{-1} for the double-, triple-, quadruple-, and quintuple-ζ BLYP recontracted sets, respectively, and 6.04, 3.83, 3.21, and 1.02 kcal mol^{-1} energy reductions for the BLYP reoptimized sets. Average energy reduction for the recontracted B3LYP sets was 3.58, 2.37, 2.01, and 0.61 kcal mol^{-1} for the double-, triple-, quadruple-, and quintuple-ζ sets, while an average energy decrease for the reoptimized B3LYP sets was 3.89, 2.39, 2.04, and 0.68 kcal mol^{-1}, respectively. In Tables II and III, the Kohn-Sham

TABLE III. Atomic ground state energies calculated with the B3LYP functional for the atoms Al-Ar are given. All energies are in hartrees (E_H).

		Basis set		
Atom	N	cc-pV(n + d)Z	cc-p[rt(BLYP)]VnZ	cc-p[rt(o-BLYP)]VnZ
Al	D	−242.382 903	−242.388 294	−242.388 605
	T	−242.389 532	−242.393 847	−242.393 831
	Q	−242.393 298	−242.395 315	−242.395 335
	5	−242.394 498	−242.395 594	−242.395 648
	P	−242.395 49	−242.396 17	−242.396 21
	S3	−242.396 11	−242.397 97	−242.397 59
Si	D	−289.388 715	−289.393 843	−289.394 424
	T	−289.396 365	−289.400 367	−289.400 426
	Q	−289.399 150	−289.402 536	−289.402 413
	5	−289.401 888	−289.402 846	−289.402 915
	P	−289.400 77	−289.403 80	−289.403 57
	S3	−289.403 10	−289.405 59	−289.405 59
P	D	−341.276 438	−341.281 882	−341.282 368
	T	−341.285 851	−341.289 617	−341.289 657
	Q	−341.288 737	−341.292 290	−341.292 357
	5	−341.291 776	−341.292 654	−341.292 727
	P	−341.290 42	−341.293 85	−341.293 93
	S3	−341.291 43	−341.295 09	−341.295 14
S	D	−398.125 166	−398.130 726	−398.131 236
	T	−398.138 734	−398.142 383	−398.141 624
	Q	−398.142 144	−398.145 673	−398.145 744
	5	−398.145 291	−398.146 142	−398.146 235
	P	−398.144 13	−398.147 59	−398.148 14
	S3	−398.144 39	−398.148 07	−398.149 21
Cl	D	−460.158 575	−460.164 632	−460.165 171
	T	−460.174 718	−460.178 323	−460.178 612
	Q	−460.178 562	−460.182 030	−460.182 102
	5	−460.181 584	−460.182 531	−460.182 668
	P	−460.180 80	−460.184 19	−460.184 13
	S3	−460.181 89	−460.184 93	−460.186 50
Ar	D	−527.542 275	−527.548 885	−527.549 486
	T	−527.559 371	−527.562 782	−527.563 296
	Q	−527.563 528	−527.566 872	−527.567 042
	5	−527.566 273	−527.567 414	−527.567 638
	P	−527.565 94	−527.569 25	−527.569 22
	S3	−527.566 78	−527.577 99	−527.578 33

limit was approximated by the double-, triple-, and quadruple-ζ energies for the Peterson three-point formula (P) and the triple- and quadruple-ζ energies for the inverse Schwartz formula, respectively (S3).

To illustrate the behavior of the cc-pV(n + d)Z, recontracted, and reoptimized sets, the atomic energies of the chlorine atom have been graphed in Figs. 1 and 2 for the BLYP and B3LYP functional, respectively. In Figs. 1 and 2, the nonconvergent behavior of the cc-pV(n + d)Z sets with the functionals is clear. The computed energy increases upon increasing the basis set size from the double ζ to triple ζ level, as is expected. There is no smooth, monotonic energy convergence with any further increase in basis

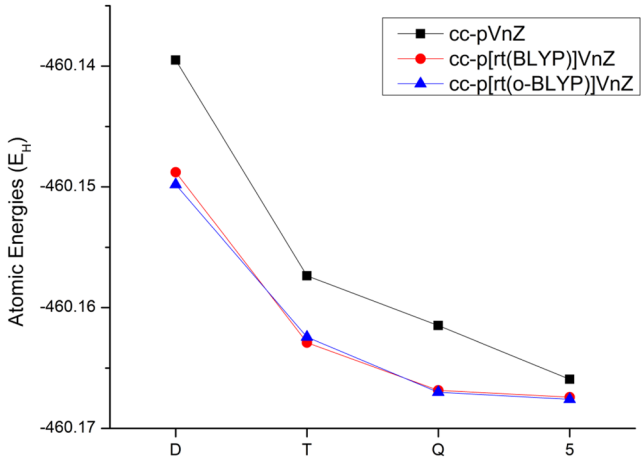

FIG. 1. Chlorine atomic energies calculated with the BLYP functional and the cc-pV(n + D)Z, cc-p[rt(BLYP)]VnZ, and cc-p[rt(*o*-BLYP)]VnZ (n = D, T, Q, 5). Energies are in hartrees (E_H).

set size, as occurs when the cc-pV(n + d)Z basis sets are used in conjunction with *ab initio* methods. However, the BLYP recontracted and reoptimized basis sets clearly show convergent behavior toward an asymptotic limit. The B3LYP functional does show curvature in the triple-, quadruple-, and quintuple-ζ cc-pV(n + d)Z basis sets, but the convergence in B3LYP is considerably slower than the convergence behavior of the recontracted and reoptimized basis sets. This is evident from the gap between the quadruple- and quintuple-ζ energies. The difference in calculated chlorine ground state energies for the cc-pV(Q + d)Z and cc-pV(5 + d)Z sets with the B3LYP functional is 1.89 kcal mol^{-1}, while the differences for the quadruple- and quintuple-ζ basis sets for the B3LYP recontracted and reoptimized sets are 0.31 and 0.34 kcal mol^{-1}, respectively.

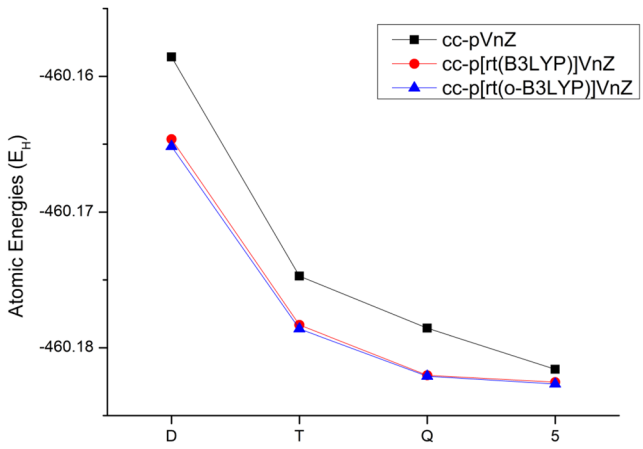

FIG. 2. Chlorine atomic energies calculated with the B3LYP functional and the cc-pV(n + D)Z, cc-p[rt(B3LYP)]VnZ, and cc-p[rt(o-B3LYP)]VnZ (n = D, T, Q, 5). Energies are in hartrees (E_H).

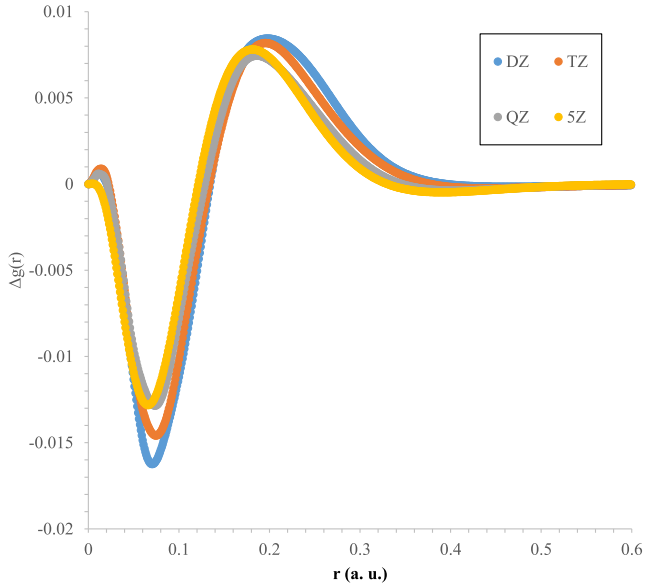

FIG. 3. Differences between the 1s phosphorous radial distribution functions [Δg(r)] at distance r (a.u.) from the nucleus calculated with the conventional cc-pV(n + d)Z and cc-p[rt(o-B3LYP)]VnZ sets are shown.

Further analysis on the effect of reoptimization of the basis sets has been performed by analyzing changes made to the radial distribution of the electrons on the ground state phosphorous atom. Figures 3–5 illustrate examples of the changes in radial electron distribution, g(r), due to reoptimization and truncation of the basis

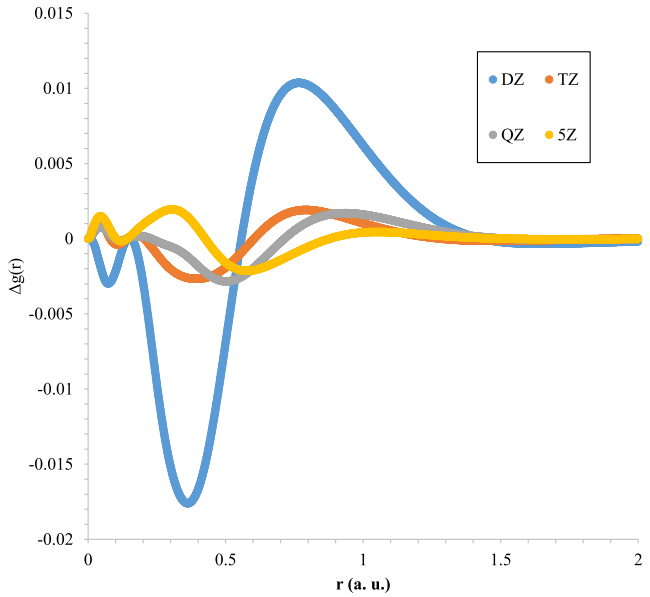

FIG. 4. Differences between the 2s phosphorous radial distribution functions [Δg(r)] at distance r (a.u.) from the nucleus calculated with the conventional cc-pV(n + d)Z and cc-p[rt(o-B3LYP)]VnZ sets are shown.

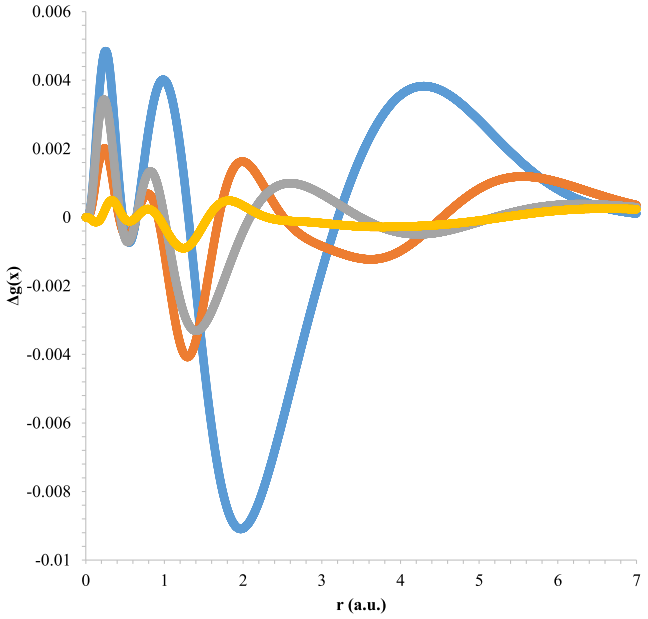

FIG. 5. Differences between the 3p phosphorous radial distribution functions [Δg(r)] at distance r (a.u.) from the nucleus calculated with the conventional cc-pV(*n* + d)Z and cc-p[rt(o-B3LYP)]V*n*Z sets are shown.

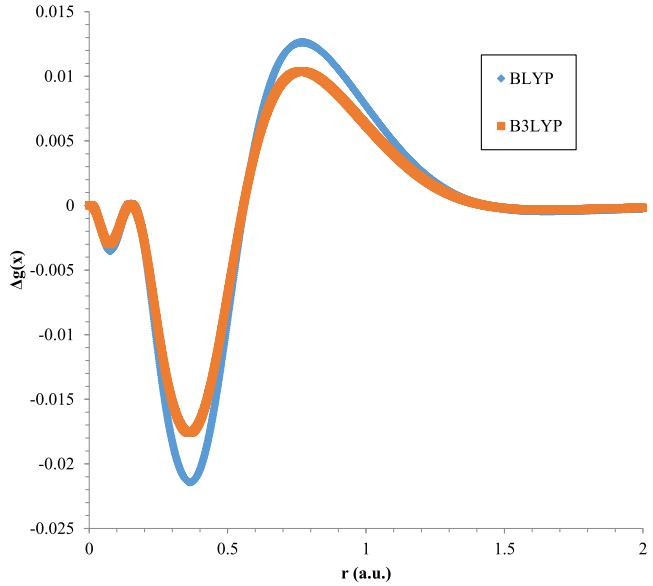

FIG. 6. The comparison between the changes in radial distribution function [Δg(r)] at distance r (a.u.) from the nucleus between the 2s phosphorous radial distribution functions calculated with the conventional cc-pV(*n* + d)Z and reoptimized cc-p[rt(o-B3LYP)]V*n*Z/cc-p[rt(o-BLYP)]V*n*Z sets is shown.

sets for density functionals. Peak changes to the BLYP and B3LYP radial distributions between conventional and reoptimized basis sets were found to be nearly identical, with changes in BLYP radial distribution found to be slightly larger than changes to B3LYP, as shown in Fig. 6. For the 1s orbitals, the BLYP and B3LYP reoptimizations show a consistent shift in radial distributions from the core region toward the valence region, but in higher energy atomic shells, there is no longer consistent behavior of the radial distribution changes. Substantial shifts in radial distributions are present for the double-ζ basis sets, where electron distribution is vacated from the mid regions of the phosphorous atom toward the core and valence regions. For triple- and quadruple-ζ basis sets, there is a distinct change between the $n = 2$ and $n = 3$ shells of the phosphorous atom, with both the 2*s* and 2*p* orbitals for triple- and quadruple-ζ following similar shifts in radial distribution as the double-ζ basis sets toward the valence region. However, for 3*s* and 3*p* orbitals, the triple- and quadruple-ζ show minor increases in the distribution at the core region but also populate the mid regions (~0.5 to 1.0 a.u. from the nucleus for the 2*s* orbital and 1–3 a.u. from the nucleus for the 2p orbital) vacated by the reoptimized double-ζ basis sets.

B. Homonuclear diatomic properties

Equilibrium bond lengths (r_e) and dissociation energies (D_e) have been calculated for the homonuclear diatomics Al_2, Si_2, P_2, S_2, and Cl_2 using the cc-pV(*n* + d)Z, cc-p[rt(λ)]V*n*Z, and cc-p[rt(o-λ)]V*n*Z basis sets for both BLYP and B3LYP functionals. The results of these calculations are found in Tables IV and V for the BLYP and B3LYP functionals, respectively. Kohn-Sham limits were approximated using the Peterson and Schwartz extrapolation formulas as indicated in Sec. III A. All experimental dissociation energies and bond lengths are found in Ref. 38, and references therein, except for Al_2, for which the experimental data are derived from the work of Fu *et al.*[39] Additionally, mean absolute deviations (MAD) from the experiment have been determined for each basis set, as well as the extrapolated Kohn-Sham limit.

The data from Tables IV and V demonstrate several key points. The behavior of BLYP and B3LYP functionals with the uncorrected cc-pV(*n* + d)Z basis sets is included to show the improvement from the recontraction and/or reoptimization of the basis sets. The errors in the BLYP/cc-pV(*n* + d)Z calculations rise sharply from double- to triple-ζ, lowered at the quadruple-ζ, and then rise again with the quintuple-ζ set. For B3LYP/cc-pV(*n* + d)Z, errors tend to drop dramatically from the double-ζ to triple-ζ and then rise with employment of the quadruple-ζ set, followed by another lowering at the quintuple-ζ set upon reoptimization of the basis sets. For B3LYP/cc-pV(*n* + d)Z calculations, though, the mean absolute errors were consistently lower than either the recontracted or reoptimized basis sets in contrast to the behavior demonstrated for the functionals in the atomic calculations. Furthermore, for the BLYP functional, both the recontracted and reoptimized functions consistently result in increasing error from experimental results.

The source of the errors produced by the reoptimized and recontracted functionals requires analysis of the trends shown by the MADs and the data in Tables IV and V. First, it is important to note that, while the atomic energies of the B3LYP/cc-pV(n + *d*)Z (uncorrected basis sets) may be closer to the KS limit value

TABLE IV. Ground state homonuclear diatomic spectroscopic constants calculated with the BLYP functional are shown. Equilibrium geometries (r_e) are given in angstroms (Å). Dissociation energies (D_e) are given in kcal mol^{-1}.

		Basis set					
		cc-pV(n + d)Z		cc-p[rt(BLYP)]VnZ		cc-p[rt(o-BLYP)]VnZ	
Molecule	n	r_e (Å)	D_e (kcal mol^{-1})	r_e (Å)	De (kcal mol^{-1})	r_e (Å)	De (kcal mol^{-1})
Al_2	D	2.796	31.668	2.796	31.493	2.796	31.243
	T	2.786	31.904	2.792	31.689	2.797	31.305
	Q	2.786	31.563	2.789	31.485	2.791	31.394
	5	2.787	31.498	2.787	31.474	2.789	31.411
	P	2.79	31.36	2.79	31.37	2.79	31.45
	S3	2.79	31.31	2.79	31.34	2.79	31.45
Expt.[a]		**2.701**	**31.7**				
Si_2	D	2.310	75.732	2.310	75.835	2.312	75.263
	T	2.300	76.812	2.301	76.594	2.304	76.160
	Q	2.298	76.437	2.298	76.383	2.300	76.208
	5	2.299	76.436	2.299	76.419	2.299	76.317
	P	2.30	76.22	2.30	76.26	2.30	76.24
	S3	2.30	76.16	2.30	76.23	2.30	76.24
Expt.[b]		**2.246**	**75.6**				
P_2	D	1.920	119.511	1.920	120.054	1.921	119.204
	T	1.911	121.714	1.913	121.529	1.913	121.277
	Q	1.910	121.852	1.911	121.836	1.911	121.576
	5	1.911	121.885	1.911	121.895	1.911	121.626
	P	1.91	121.93	1.91	122.01	1.91	121.75
	S3	1.91	121.95	1.91	122.06	1.91	121.79
Expt.[b]		**1.893**	**117.2**				
S_2	D	1.941	106.677	1.941	106.272	1.943	105.686
	T	1.929	107.625	1.930	107.652	1.932	107.094
	Q	1.927	107.865	1.927	107.852	1.928	107.407
	5	1.927	107.908	1.927	107.934	1.927	107.620
	P	1.93	108.01	1.93	107.97	1.93	107.59
	S3	1.93	108.04	1.93	108.00	1.93	107.63
Expt.[b]		**1.889**	**102.9**				
Cl_2	D	2.059	55.900	2.066	54.930	2.063	55.139
	T	2.042	58.126	2.042	58.322	2.044	58.072
	Q	2.039	58.365	2.039	58.408	2.041	58.057
	5	2.039	58.470	2.039	58.543	2.040	58.222
	P	2.04	58.50	2.04	58.46	2.04	58.05
	S3	2.04	58.54	2.04	58.47	2.04	60.21
Expt.[b]		**1.987**	**59.7**				

[a]Reference 39.
[b]Reference 38.

TABLE V. Ground state homonuclear diatomic properties calculated with the B3LYP functional are shown. Equilibrium geometries (r_e) are given in angstroms (Å). Dissociation energies (D_e) are given in kcal mol^{-1}.

		Basis set					
		cc-pV(n + d)Z		cc-p[rt(B3LYP)]VnZ		cc-p[rt(o-B3LYP)]VnZ	
Molecule	N	r_e (Å)	D_e (kcal mol^{-1})	r_e (Å)	D_e (kcal mol^{-1})	r_e (Å)	D_e (kcal mol^{-1})
Al_2	D	2.760	30.907	2.760	30.742	2.760	30.330
	T	2.753	31.260	2.756	31.103	2.762	30.504
	Q	2.752	31.070	2.753	30.999	2.754	30.929
	5	2.753	31.014	2.753	31.002	2.754	30.952
	P	2.75	30.96	2.75	30.94	2.75	31.18
	S3	2.75	30.93	2.75	30.92	2.75	31.24
Expt.[a]		**2.701**	**31.7**				
Si_2	D	2.276	73.523	2.276	73.597	2.277	72.724
	T	2.267	74.904	2.268	74.739	2.273	73.687
	Q	2.264	74.754	2.266	74.683	2.267	74.512
	5	2.265	74.744	2.265	74.735	2.266	74.715
	P	2.26	74.67	2.26	74.65	2.26	74.81
	S3	2.26	74.65	2.26	74.64	2.26	74.91
Expt.[b]		**2.246**	**75.6**				
P_2	D	1.897	113.108	1.897	113.505	1.898	112.934
	T	1.889	115.808	1.890	115.631	1.890	115.678
	Q	1.887	116.121	1.888	116.062	1.888	115.838
	5	1.888	116.137	1.888	116.145	1.888	115.910
	P	1.89	116.30	1.89	116.31	1.89	115.93
	S3	1.89	116.35	1.89	116.38	1.89	115.95
Expt.[b]		**1.893**	**117.2**				
S_2	D	1.913	101.195	1.913	100.848	1.912	100.333
	T	1.903	103.193	1.904	103.184	1.906	102.549
	Q	1.901	103.566	1.901	103.532	1.902	103.024
	5	1.901	103.638	1.900	103.658	1.901	103.296
	P	1.90	103.78	1.90	103.73	1.90	103.30
	S3	1.90	103.84	1.90	103.79	1.90	103.37
Expt.		**1.889**	**102.9**				
Cl_2	D	2.028	52.093	2.033	51.208	2.031	51.094
	T	2.012	55.294	2.012	55.446	2.014	55.133
	Q	2.009	55.654	2.009	55.680	2.012	55.291
	5	2.009	55.798	2.009	55.855	2.010	55.494
	P	2.01	55.86	2.01	55.82	2.01	55.38
	S3	2.01	55.92	2.01	55.85	2.01	55.41
Expt.[b]		**1.987**	**59.7**				

[a]Reference 39.
[b]Reference 38.

[particularly at the cc-pV(T + *d*)Z basis set level] than the recontracted and reoptimized basis sets, the atomic energies computed with cc-pV(n + *d*)Z basis sets do not result in a smooth, monotonic convergence toward the Kohn-Sham limit. This may stem from a cancelation of errors between the basis set and density functional approximation. Thus, though the errors in the individual recontracted and reoptimized basis sets tend to produce larger errors when coupled with the B3LYP functional, smooth, monotonic convergence of atomic energies is achieved and thus the Kohn-Sham limit is able to be approximated with the reoptimized basis sets.

C. Enthalpies of formation

Enthalpies of formation at zero kelvin [ΔH_f^0 (0 K)] were calculated employing the B3LYP and BLYP functionals in conjunction with conventional cc-pV*n*Z and cc-pV(*n* + d)Z basis sets for first and second row atoms, respectively, as well as the cc-p[rt(*λ*)]V*n*Z, and the cc-p[rt(o-*λ*)]V*n*Z basis sets. cc-p[rt(*λ*)]V*n*Z and cc-p[rt(o-*λ*)]V*n*Z basis sets of Gibson[20] are used for hydrogen and the first row atoms (H, B-Ne). Geometry optimizations were performed with each basis set and functional pairing to determine ground state molecular geometries. The results of these calculations are found in Tables VI and VII. All experimental enthalpies of formation are obtained from the NIST-JANAF thermochemical data tables.[40]

In general, enthalpies calculated using the recontracted and reoptimized basis sets are further from the experimental value. This may be due to cancelation of errors, in which the uncorrected basis sets have an error that is offset by an error in the density functional method. Calculated B3LYP enthalpies of formation deviate from the conventional correlation consistent sets by an average of 1.90, 0.36, 0.48, and 0.52 kcal mol^{-1} for the recontracted double-, triple-, quadruple-, and quintuple-ζ basis sets, respectively, while the reoptimized sets deviate from the conventional correlation consistent basis sets by an average of 1.66, 1.47, 1.27, and 0.71 kcal mol^{-1} for the double-, triple-, quadruple-, and quintuple-ζ basis sets, respectively. For the BLYP functional, calculated enthalpies of formation deviate from the conventional correlation consistent basis sets by 7.79, 0.38, 0.46, and 1.72 kcal mol^{-1} for the double-, triple-, quadruple-, and quintuple-ζ recontracted basis sets, respectively, while the reoptimized basis sets deviate from conventional correlation consistent sets by an average of 3.25, 1.84, 1.64, and 0.71 kcal mol^{-1} for the double-, triple-, quadruple-, and quintuple-ζ basis sets, respectively.

However, it is clear from Tables VI and VII that the use of conventional correlation consistent basis sets consistently fails to yield convergent behavior for all calculated enthalpies of formation

TABLE VI. Enthalpies of formation at zero kelvin [ΔH_f^0 (0 K)] calculated with the B3LYP functional are shown. Units are given in kcal mol^{-1}. cc-pV(*n* + d)Z and cc-pV*n*Z basis sets are used for second row atoms (Al-Ar) and first row atoms (B-Ne), respectively.

		Basis set		
		cc-pV(*n* + d)Z/cc-pV*n*Z	cc-p[rt(B3LYP)]V*n*Z	cc-p[rt(o-B3LYP)]V*n*Z
Molecule	*N*	ΔH_f^0 (0 K) (kcal mol^{-1})	ΔH_f^0 (0 K) (kcal mol^{-1})	ΔH_f^0 (0 K) (kcal mol^{-1})
AlF_3	D	−263.440	−262.591	−261.381
	T	−275.430	−275.817	−272.430
	Q	−278.644	−277.902	−276.348
	5	−277.438	−277.063	−276.769
	P	...	...	−278.63
	S3	...	...	−279.21
$AlCl_3$	D	−119.762	−118.926	−120.952
	T	−125.252	−125.023	−123.664
	Q	−126.099	−125.463	−124.775
	5	−125.865	−125.421	−124.888
	P	...	...	−125.42
	S3	...	...	−125.13
$SiCl_4$	D	−130.325	−128.548	−130.242
	T	−137.667	−137.637	−136.148
	Q	−138.470	−137.654	−137.157
	5	−138.447	−137.755	−137.406
	P	...	−137.66	−137.74
	S3	...	−137.67	−137.90

TABLE VI. (*Continued.*)

		Basis set		
		cc-pV(n + d)Z/cc-pVnZ	cc-p[rt(B3LYP)]VnZ	cc-p[rt(o-B3LYP)]VnZ
Molecule	N	ΔH_f^0 (0 K) (kcal mol^{-1})	ΔH_f^0 (0 K) (kcal mol^{-1})	ΔH_f^0 (0 K) (kcal mol^{-1})
PF_3	D	−202.422	−200.811	−198.328
	T	−222.021	−222.428	−220.369
	Q	−224.138	−223.580	−222.710
	5	−223.729	−222.973	−222.884
	P	...	−224.24	−224.06
	S3	...	−224.42	−224.42
SO_2	D	−43.685	−45.224	−45.306
	T	−62.294	−62.852	−61.154
	Q	−64.446	−64.131	−63.136
	5	−64.975	−64.314	−64.210
	P	−65.69	−64.87	−64.28
	S3	−66.02	−65.06	−64.58
SO_3	D	−57.615	−58.910	−58.975
	T	−82.582	−83.106	−80.306
	Q	−84.690	−84.050	−82.342
	5	−85.024	−83.935	−83.829
	P	...	...	−83.52
	S3	...	...	−83.83
ClF_3	D	−8.974	−8.022	−8.084
	T	−21.328	−21.605	−21.887
	Q	−23.655	−23.196	−23.161
	5	−23.842	−23.378	−23.422
	P	−25.01	−24.12	−23.90
	S3	−25.35	−24.36	−24.09
CS_2	D	31.589	32.081	32.757
	T	29.125	29.065	30.229
	Q	28.606	28.861	29.199
	5	28.625	28.856	28.995
	P	...	28.74	28.60
	S3	...	28.71	28.45
COS	D	−29.040	−25.448	−27.319
	T	−32.603	−32.398	−31.479
	Q	−33.355	−32.994	−32.492
	5	−33.066	−32.820	−32.713
	P	...	...	−33.08
	S3	...	...	−33.23
NOCl	D	12.318	19.414	15.741
	T	10.627	11.522	11.368
	Q	9.995	10.262	10.782
	5	10.206	10.445	10.640
	P	...	...	10.44
	S3	...	...	10.35

TABLE VII. Enthalpies of formation at zero kelvin [ΔH_f^0 (0 K)] calculated with the BLYP functional are shown. Units are given in kcal mol^{-1}. cc-pV(n + d)Z and cc-pVnZ basis sets are used for second row atoms (Al-Ar) and first row atoms (B-Ne), respectively.

		Basis set		
		cc-pV(n + d)Z/cc-pVnZ	cc-p[rt(BLYP)]VnZ	cc-p[rt(o-BLYP)]VnZ
Molecule	n	ΔH_f^0 (0 K) (kcal mol^{-1})	ΔH_f^0 (0K) (kcal mol^{-1})	ΔH_f^0 (0K) (kcal mol^{-1})
AlF_3	D	−274.038	−272.759	−267.918
	T	−282.156	−282.400	−277.618
	Q	−284.107	−283.318	−280.872
	5	−282.149	−281.791	−281.265
	P	...	...	−282.77
	S3	...	...	−283.25
$AlCl_3$	D	−116.951	−115.976	−116.377
	T	−121.063	−120.745	−119.258
	Q	−121.586	−120.931	−119.888
	5	−121.243	−120.765	−120.221
	P	...	...	−120.25
	S3	...	...	−120.35
$SiCl_4$	D	−128.074	−126.027	−125.533
	T	−133.053	−133.047	−131.284
	Q	−133.431	−132.661	−131.948
	5	−133.318	−132.627	−132.163
	P	...	...	−132.33
	S3	...	...	−132.43
PF_3	D	−217.941	−215.966	−210.311
	T	−232.221	−232.683	−229.738
	Q	−233.506	−232.996	−231.532
	5	−232.486	−231.799	−231.587
	P	...	...	−232.57
	S3	...	...	−232.84
SO_2	D	−63.512	−64.724	−62.664
	T	−78.360	−79.098	−77.191
	Q	−80.109	−79.894	−78.490
	5	−80.318	−79.728	−79.635
	P	−81.12	...	−79.24
	S3	−81.39	...	−79.44
SO_3	D	−82.935	−83.724	−80.391
	T	−102.495	−103.302	−99.869
	Q	−103.931	−103.424	−101.021
	5	−103.717	−102.731	−102.642
	P	...	...	−101.68
	S3	...	...	−101.86

TABLE VII. (*Continued.*)

		Basis set		
		cc-pV(n + d)Z/cc-pVnZ	cc-p[rt(BLYP)]VnZ	cc-p[rt(o-BLYP)]VnZ
Molecule	n	ΔH_f^0 (0 K) (kcal mol^{-1})	ΔH_f^0 (0K) (kcal mol^{-1})	ΔH_f^0 (0K) (kcal mol^{-1})
ClF_3	D	−47.249	−46.110	−45.509
	T	−55.341	−55.750	−55.296
	Q	−56.879	−56.512	−56.278
	5	−56.663	−56.339	−56.343
	P	...	...	−56.85
	S3	...	...	−57.00
CS_2	D	21.753	21.700	24.175
	T	20.549	20.427	21.847
	Q	20.201	20.433	20.930
	5	20.316	20.540	20.624
	P	...	...	20.40
	S3	...	...	20.26
COS	D	−41.792	−103.663	−38.626
	T	−43.630	−43.561	−42.120
	Q	−44.073	−43.716	−42.902
	5	−43.510	−56.166	−43.106
	P	...	...	−43.36
	S3	...	...	−43.47
NOCl	D	−10.602	−4.003	−5.715
	T	−10.180	−9.579	−9.010
	Q	−10.449	−10.249	−9.429
	5	−9.963	−9.777	−9.589
	P	...	...	−9.67
	S3	...	...	−9.74

with the exception of SO_2, SO_3, and ClF_3 for the B3LYP functional and SO_2 for the BLYP functional. Additionally, as noted in previous studies, the conventional correlation consistent basis sets in conjunction with density functional methods do not show rapid convergence toward the Kohn-Sham limit.[9,41,42] The convergence behavior of the remaining enthalpies of formation in general shows a peak occurring with the quadruple-ζ basis sets, with an inversion in the convergence behavior then occurring with the subsequent quintuple-ζ calculated enthalpies of formation. This convergence behavior persists in the use of the recontracted basis sets as well. Only when the reoptimized cc-p[rt(o-λ)]VnZ basis sets are used with the paired functional is convergence of the molecular enthalpies of formation consistently demonstrated across both molecules and functionals. While all atomic energies and diatomic constants demonstrate convergence to the KS limit, the molecular enthalpies do not converge for the uncorrected cc-pV(n + d)Z basis sets, and in some cases, such as AlF_3 and $AlCl_3$, smooth monotonic convergence only occurs for the reoptimized cc-p[rt(o-λ)]VnZ basis sets. An illustration of this convergence behavior is shown in Fig. 7, where the calculated enthalpies of formation of carbonyl sulfide (COS) using the conventional correlation consistent basis sets, recontracted basis sets, and reoptimized basis sets with the B3LYP functional are shown. The calculated enthalpies of formation with the reoptimized sets show smooth convergent behavior toward the Kohn-Sham limit, while the conventional basis sets and recontracted basis sets both show nonmonotonic convergence. Furthermore, the enthalpies of formation calculated with the conventional quadruple-ζ basis sets exceed both of the estimated Kohn-Sham limits of −33.08 and −33.23 kcal mol^{-1}—extrapolated using the reoptimized basis sets using the Peterson and Schwartz extrapolation schemes, respectively.

The inability of the conventional double-, triple-, and quadruple-basis sets to produce enthalpies of formation which show smooth, monotonic convergence to the Kohn-Sham limit is further illustrated by the calculated enthalpies of formation for the NOCl molecule and the BLYP functional, shown in Fig. 8.

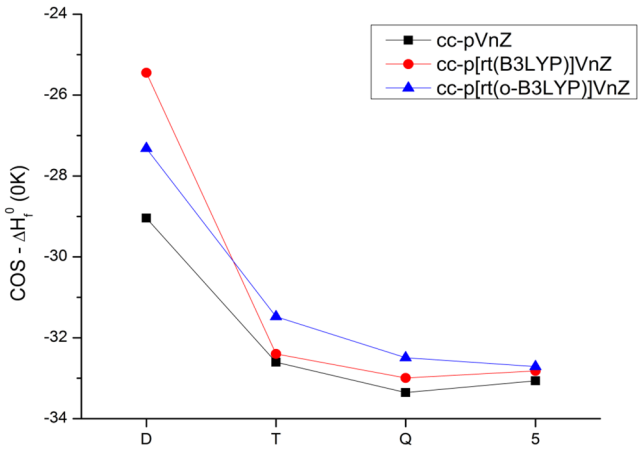

FIG. 7. Enthalpies of formation at zero kelvin calculated for the COS molecule with the B3LYP functional and the cc-pV(n + D)Z, cc-p[rt(B3LYP)]VnZ, and cc-p[rt(o-B3LYP)]VnZ (n = D, T, Q, 5). Units are in kcal mol^{-1}.

The conventional correlation consistent basis sets fail to show any convergence behavior in the calculated enthalpies of formation, instead demonstrating an undulating rise in calculated enthalpies of formation, with the calculated enthalpies of formation for all the conventional basis sets below the estimated Kohn-Sham limits of −9.672 and −9.735 kcal mol^{-1}—extrapolated using the reoptimized basis sets using the Peterson and Schwartz extrapolation schemes, respectively. Convergence behavior shows improvement with the recontracted basis sets but the calculated enthalpies of formation with the recontracted sets still fail to produce monotonic convergence behavior. Furthermore, the calculated quadruple- and quintuple-ζ enthalpies of formation using the recontracted basis sets also exceed the estimated Kohn-Sham limits.

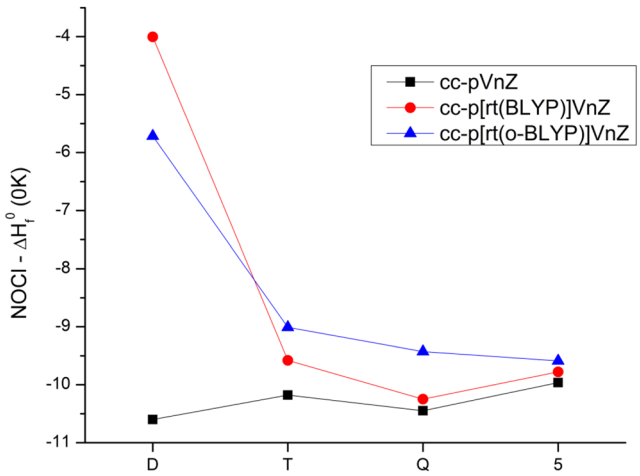

FIG. 8. Enthalpies of formation at zero kelvin calculated for the NOCl molecule with the BLYP functional and the cc-pV(n + D)Z, cc-p[rt(B3LYP)]VnZ, and cc-p[rt(o-B3LYP)]VnZ (n = D, T, Q, 5). Units are in kcal mol^{-1}.

D. CPU efficiency comparison

Comparison between the central processing unit (CPU) resource efficiencies of the conventional correlation consistent basis sets and the recontracted and reoptimized basis sets was performed by determining the percentage CPU time savings based upon single point energy calculations done in series for all molecules examined in Sec. III C using a Dell OptiPlex 390 with 8 GB DDR3 memory. Geometries for the single-point calculations were taken from B3LYP geometry optimizations using the cc-pVTZ and cc-pV(T + d)Z basis sets. The percentage CPU time savings provided by the use of the recontracted and reoptimized basis sets compared to conventional correlation consistent basis sets is shown in Table VIII.

The truncation of the *g*- and *h*-functions from the correlation consistent basis sets has a considerable effect on the required CPU time to determine single-point energies. For the B3LYP functional, the recontracted and reoptimized quadruple-ζ basis sets require approximately 51% less CPU time than calculations using conventional quadruple-ζ correlation consistent basis sets, while the recontracted and reoptimized quintuple-ζ basis sets require approximately 91% less CPU time compared to the conventional quintuple-ζ basis sets. There is a slight increase in CPU time savings when the BLYP functional is used, with quadruple- and quintuple-ζ recontracted and reoptimized basis sets requiring approximately 53% and 97% less CPU time than the conventional correlation consistent basis sets, respectively. For both B3LYP and BLYP functionals, there is not a significant time difference in employing recontracted and reoptimized double-ζ and triple-ζ basis sets compared to conventional correlation consistent basis sets.

For both B3LYP and BLYP functionals, the amount of CPU time required for single-point calculations using the recontracted (cc-p[rt(λ)]V5Z) and reoptimized (cc-p[rt(o-λ)]V5Z) quintuple-ζ basis sets is comparable to the time required for calculations using conventional correlation consistent quadruple-ζ (cc-pVQZ) basis sets. For B3LYP single point calculations, the recontracted

TABLE VIII. Percentage CPU time savings for the 10 molecular single point energies calculated using Gaussian09. Percentage differences are calculated by comparing the CPU time required by conventional correlation consistent basis sets and the recontracted and reoptimized basis sets. B3LYP/cc-pVTZ geometries were used for all calculations.

		Basis set	
Functional	*n*	cc-p[rt(λ)]V*n*Z (%)	cc-p[rt(o-λ)]V*n*Z (%)
B3LYP			
	D	...	...
	T	...	...
	Q	49.66	52.03
	5	90.82	92.18
BLYP			
	D	...	...
	T	...	...
	Q	52.36	54.09
	5	96.77	97.11

and reoptimized quintuple-ζ basis sets require only an average of 18% and 5% more CPU time, respectively, than the conventional quadruple-ζ basis sets. For BLYP calculations, the recontracted and reoptimized quintuple-ζ basis sets require an average of 3.5% and 6.3% *less* CPU time than conventional quadruple-ζ basis sets.

IV. CONCLUSIONS

Two modified basis set series have been considered for density functional methods. These basis sets, the recontracted and truncated cc-pV[rt(BLYP)]*n*Z and cc-pV[rt(B3LYP)]*n*Z sets and the recontracted, reoptimized, and truncated cc-pV[rt(*o*-BLYP)]*n*Z and cc-pV[rt(o-B3LYP)]*n*Z sets, are compact and robust. These basis sets demonstrate systematic convergence to the Kohn-Sham limit overall, for both generalized gradient approximation (GGA) and hybrid functionals. The convergent behavior of these functionals will allow for parameterization of density functionals in the absence of basis set effects and allow for reliable extrapolation of molecular properties to the Kohn-Sham limit.

The calculated atomic energies for recontracted and reoptimized correlation consistent sets demonstrate clearly superior convergent behavior toward the Kohn-Sham limit. The mean absolute errors calculated with reoptimized, truncated basis sets for homonuclear diatomic dissociation energies not only show reliable convergence toward the Kohn-Sham limit but extrapolations to this limit via common extrapolation schemes also show substantial improvements to the dissociation energies compared to calculations using conventional cc-pV(n + d)Z basis sets. These improvements occur for both GGA and hybrid DFT functionals. The calculated enthalpies of formation using conventional, recontracted, and reoptimized correlation consistent basis sets show that beyond homonuclear diatomic species, smooth, monotonic convergence to Kohn-Sham limit is only consistently achieved through the combination of the reoptimized basis sets with either the BLYP or B3LYP functional (depending on the functional for which the basis sets were designed).

SUPPLEMENTARY MATERIAL

See supplementary material for recontracted and reoptimized basis sets used in this study.

ACKNOWLEDGMENTS

This material is based upon work supported by the National Science Foundation under Grant No. CHE-1362479/DMR-1636557. Computational resources were provided via the NSF Major Research Instrumentation program supported by the National Science Foundation under Grant No. CHE-1531468.

REFERENCES

[1] W. Kohn and L. J. Sham, Phys. Rev. **140**, A1133 (1965).
[2] R. Peverati and D. G. Truhlar, Philos. Trans. R. Soc., A **372**, 20120476 (2014).
[3] J. J. Determan, S. Moncho, E. N. Brothers, and B. G. Janesko, J. Phys. Chem. C **118**, 15693 (2014).
[4] J. K. Norskov, F. Abild-Pedersen, F. Studt, and T. Bligaard, Proc. Natl. Acad. Sci. U. S. A. **108**, 937 (2011).
[5] J. P. Perdew and A. Ruzsinszky, Int. J. Quantum Chem. **110**, 2801 (2010).
[6] A. D. Becke, J. Chem. Phys. **140**, 18A301 (2014).
[7] A. Pribram-Jones, D. A. Gross, and K. Burke, Annu. Rev. Phys. Chem. **66**, 283 (2015).
[8] J. J. Determan, K. Poole, G. Scalmani, M. J. Frisch, B. G. Janesko, and A. K. Wilson, J. Chem. Theory Comput. **13**, 4907 (2017).
[9] N. X. Wang and A. K. Wilson, J. Phys. Chem. A **109**, 7187 (2005).
[10] N. X. Wang, K. Venkatesh, and A. K. Wilson, J. Phys. Chem. A **110**, 779 (2006).
[11] N. X. Wang and A. K. Wilson, J. Chem. Phys. **121**, 7632 (2004).
[12] N. X. Wang and A. K. Wilson, Mol. Phys. **103**, 345 (2005).
[13] N. X. Wang and A. K. Wilson, J. Phys. Chem. A **107**, 6720 (2003).
[14] F. Jensen, J. Chem. Phys. **118**, 2459 (2003).
[15] F. Jensen, J. Chem. Phys. **115**, 9113 (2001).
[16] F. Jensen, J. Chem. Phys. **116**, 7372 (2002).
[17] F. Jensen, J. Chem. Phys. **117**, 9234 (2002).
[18] C. Kumar, H. Fliegl, F. Jensen, A. M. Teale, S. Reine, and T. Kjærgaard, Int. J. Quantum Chem. **118**, e25639 (2018).
[19] B. P. Prascher and A. K. Wilson, Mol. Phys. **105**, 2899 (2007).
[20] J. S. Gibson, "From Development of Semi-empirical Atomistic Potentials to Application of Correlation Consistent Basis Sets," Ph.D. dissertation (University of North Texas, 2014).
[21] T. H. Dunning, Jr., K. A. Peterson, and A. K. Wilson, J. Chem. Phys. **114**, 9244 (2001).
[22] J. M. L. Martin, J. Chem. Phys. **108**, 2791 (1998).
[23] J. M. L. Martin and O. Uzan, Chem. Phys. Lett. **282**, 16 (1998).
[24] C. W. Bauschlicher and H. Partridge, Chem. Phys. Lett. **240**, 533 (1995).
[25] C. W. Bauschlicher and A. Ricca, J. Phys. Chem. A **102**, 8044 (1998).
[26] A. D. Becke, Phys. Rev. A **38**, 3098 (1988).
[27] C. Lee, W. Yang, and R. G. Parr, Phys. Rev. B **37**, 785 (1988).
[28] A. Becke, J. Chem. Phys. **98**, 5648 (1993).
[29] H.-J. Werner, P. Knowles, G. Knizia, F. Manby, and M. Schütz, Wiley Interdiscip. Rev.: Comput. Mol. Sci. **2**, 242 (2012).
[30] M. J. Frisch, G. W. Trucks, H. B. Schlegel, G. E. Scuseria, M. A. Robb, J. R. Cheeseman, G. Scalmani, V. Barone, B. Mennucci, G. A. Petersson, H. Nakatsuji, M. Caricato, X. Li, H. P. Hratchian, A. F. Izmaylov, J. Bloino, G. Zheng, J. L. Sonnenberg, M. Hada, M. Ehara, K. Toyota, R. Fukuda, J. Hasegawa, M. Ishida, T. Nakajima, Y. Honda, O. Kitao, H. Nakai, T. Vreven, J. A. Montgomery, J. E. Peralta, F. Ogliaro, M. Bearpark, J. J. Heyd, E. Brothers, K. N. Kudin, V. N. Staroverov, R. Kobayashi, J. Normand, K. Raghavachari, A. Rendell, J. C. Burant, S. S. Iyengar, J. Tomasi, M. Cossi, N. Rega, J. M. Millam, M. Klene, J. E. Knox, J. B. Cross, V. Bakken, C. Adamo, J. Jaramillo, R. Gomperts, R. E. Stratmann, O. Yazyev, A. J. Austin, R. Cammi, C. Pomelli, J. W. Ochterski, R. L. Martin, K. Morokuma, V. G. Zakrzewski, G. A. Voth, P. Salvador, J. J. Dannenberg, S. Dapprich, A. D. Daniels, Ö. Farkas, J. B. Foresman, J. V Ortiz, J. Cioslowski, and D. J. Fox, GAUSSIAN 09, Revision B.01, Gaussian, Inc., Wallingford, CT, 2009.
[31] M. W. Schmidt, K. K. Baldridge, J. A. Boatz, S. T. Elbert, M. S. Gordon, J. H. Jensen, S. Koseki, N. Matsunaga, K. A. Nguyen, S. Su, T. L. Windus, M. Dupuis, and J. A. Montgomery, J. Comput. Chem. **14**, 1347 (1993).
[32] M. S. Gordon and M. W. Schmidt, in *Theory and Applications of Computational Chemistry First Forty Years*, edited by C. E. Dykstra, G. Frenking, K. S. Kim, and G. E. Scuseria (Elsevier, Amsterdam, 2005), pp. 1167–1189.
[33] B. P. Prascher, B. R. Wilson, and A. K. Wilson, J. Chem. Phys. **127**, 124110 (2007).
[34] R. C. Raffenetti, J. Chem. Phys. **58**, 4452 (1973).
[35] T. H. Dunning, J. Chem. Phys. **90**, 1007 (1989).
[36] K. A. Peterson, D. E. Woon, and T. H. Dunning, J. Chem. Phys. **100**, 7410 (1994).
[37] C. Schwartz, Phys. Rev. **126**, 1015 (1962).
[38] K. P. Huber and G. Herzberg, *Molecular Spectra and Molecular Structure 4*, Constants of Diatomic Molecules (Van Nostrand, Princeton, 1979).
[39] Z. Fu, G. W. Lemire, G. A. Bishea, and M. D. Morse, J. Chem. Phys. **93**, 8420 (1990).
[40] M. W. Chase, J. Phys. Chem. Ref. Data **25**, 551 (1996).
[41] J. Witte, J. B. Neaton, and M. Head-Gordon, J. Chem. Phys. **144**, 194306 (2016).
[42] F. Jensen, J. Phys. Chem. A **121**, 6104 (2017).